Effects of Alternating Current (AC) and Direct Current (DC) in Electrocoagulation Process for the Removal of iron from Water

Subramanyan Vasudevan*

CSIR, Central Electrochemical Research Institute, Karaikudi 630 006, India

In practice, direct current (DC) is used in an electrocoagulation processes. In this case, an impermeable oxide layer may form on the cathode as well as corrosion formation on the anode due to oxidation. This prevents the effective current transfer between the anode and cathode, so the efficiency of electrocoagulation processes declines. These disadvantages of DC have been diminished by adopting alternating current (AC) in electrocoagulation processes. The main objective of this study is to investigate the effects of AC and DC on the removal of iron from water using zinc as anode and cathode. The results showed that the optimum removal efficiency of 99.6% and 99.1% with the energy consumption of 0.625 and 0.991 kWh kL^{-1} was achieved at a current density of 0.06 A dm^{-2}, at pH of 7.0 using AC and DC, respectively. For both AC and DC, the adsorption of iron was preferably fitting Langmuir adsorption isotherm, the adsorption process follows second order kinetics and the temperature studies showed that adsorption was exothermic and spontaneous in nature.

Keywords: electrocoagulation, alternating/direct current, iron removal, adsorption kinetics, isotherms

INTRODUCTION

Next to hardness, the presence of iron is probably the most common water problem faced by consumers and water professionals. Iron is commonly present in ground water worldwide. In India, severe groundwater contamination by iron has been reported (Das et al., 2003; Mahanta et al., 2004; Sharma et al., 2005; Subba Rao, 2007) by several states like Andhra Pradesh, Assam, Chhattisgarh, Karnataka and Orissa. Localised pockets are observed in states like Bihar, Jharkhand, Kerala, Punjab, Kerala, Maharastra, Madhya Pradesh, North Eastern States, Rajasthan, Tamilnadu and Uttar Pradesh. The presence of iron in the drinking water is not harmful to human health, however, it is undesirable. Bad taste, discolouration, staining and high turbidity are some of the aesthetic problems associated with iron. Based on the above considerations, the World Health Organisation (WHO) recommends that the iron contamination in drinking water should be less than 0.3 mg L^{-1} (WHO, 1996). The European Commission directive recommends that the iron in water supplies should be less than 0.2 mg L^{-1} (OJEC, 1998). The Indian discharge limit for iron is 0.3 mg L^{-1} (CPCB, 2008).

Iron usually exists in two oxidation states, reduced soluble divalent Ferrous (Fe^{2+}) and oxidised trivalent Ferric (Fe^{3+}). Several methods, namely oxidation–precipitation–filtration, lime softening, ion-exchange, activated carbon and other filtration materials, adsorption, bioremediation, supercritical fluid extraction, use of aerated granular filter, sub-surface iron removal and membrane processes have been employed for iron removal from groundwater (Ellis et al., 2000; Berbenni et al., 2002; Andersen and Bruno, 2003; Vaaramaa and Lehto, 2003; Aziz et al., 2004; Cho, 2005; Munter et al., 2005; Gupta et al., 2006, 2008, 2009; Gupta and Rastogi, 2008; Gupta and Suhas, 2009; Das et al., 2007; Ali and Gupta, 2008; Ali et al., 2007). The most commonly used methods for the removal of iron are oxidation–precipitation–filtration, ion exchange, lime softening and membrane processes. In the case of ion exchange process the limitations like cost of resin, regeneration and waste disposal prevent the process uneconomical. Further, the major difficulty in using this method is that if any oxidation occurs during the process the resulting precipitate can coat and foul the ion exchange media. Oxidation followed

*Author to whom correspondence may be addressed.
E-mail address: vasudevan65@gmail.com
Can. J. Chem. Eng. 9999:1–10, 2011

DOI 10.1002/cjce.20625
Published online in Wiley Online Library (wileyonlinelibrary.com).

by precipitation and filtration is a relatively simple process. But ineffective in the case of high iron concentration, low pH and if iron is a complex. Addition of lime causes the pH to rise up to 11–12. High maintenance costs and more space requirements are the drawbacks of the process. Membrane process has emerged as a preferred alternative to provide safe drinking water. Due to disadvantages like high cost of membrane, brine disposal and post-treatment of water prevent the process uneconomical.

Recent research has demonstrated that electrochemistry offers an attractive alternative to above-mentioned traditional methods for treating wastewaters (Carlos et al., 2006; Christensen et al., 2006; Gabrielli et al., 2006; Miwa et al., 2006; Carlesi Jara et al., 2007; Ikematsu et al., 2007; Onder et al., 2007). Electrochemical coagulation, which is one of these techniques, is the electrochemical production of destabilisation agents that brings about charge neutralisation for pollutant removal and it has been used for water or wastewater treatment. Usually, aluminum, zinc or iron plates are used as electrodes in the electrocoagulation process. Electrochemically generated metallic ions from these electrodes can undergo hydrolysis near the anode to produce a series of activated intermediates that are able to destabilise the finely dispersed particles present in the water/wastewater to be treated. The destabilised particles then aggregate to form flocs (Chen et al., 2002).

(i) When zinc is used as anode, the reactions are as follows:

At the cathode:

$$2H_2O + 2e^- \rightarrow H_2(g) + 2OH^- \quad (1)$$

At the anode:

$$Zn \rightarrow Zn^{2+} + 2e^- \quad (2)$$

In the solution:

$$Zn^{2+}(aq) + 2H_2O(l) \rightarrow Zn(OH)_2 + 2H^+(aq) \quad (3)$$

(ii) When aluminum is used as anode, the reactions are as follows:

At the cathode:

$$2H_2O + 2e^- \rightarrow H_2(g) + 2OH^- \quad (4)$$

At the anode:

$$Al \rightarrow Al^{3+} + 3e^- \quad (5)$$

In the solution:

$$Al^{3+}(aq) + 3H_2O \rightarrow Al(OH)_3 + 3H^+(aq) \quad (6)$$

The advantages of electrocoagulation include high particulate removal efficiency, compact treatment facility, relatively low cost and possibility of complete automation. This method is characterised by reduced sludge production, minimum requirement of chemicals and ease of operation (Adhoum and Monser, 2004; Chen, 2004). Although, there are numerous reports related to electrochemical coagulation as a means of removal of many pollutants from water and wastewater using aluminum as anode material, but there are limited work on iron removal by electrochemical method using zinc as anode material and its adsorption and kinetics studies. The main disadvantage in case of aluminum electrode is the residual aluminum (The USEPA guidelines suggest maximum contamination is 0.05–0.2 mg L^{-1}) present in the treated water due to well known cathodic dissolution. This will create health problems like cancer. In the case of zinc electrodes, there is no such disadvantage like aluminum electrodes. Because the USEPA guidelines suggest maximum guidelines value of aluminum in water is 5 mg L^{-1}.

Usually, direct current (DC) is used in an electrocoagulation processes. In this case, an impermeable oxide layer may form on the cathode as well as corrosion formation on the anode due to oxidation. These prevent the effective current transport between the anode and cathode, so the efficiency of electrocoagulation processes declines. These disadvantages of DC have been overcome by adopting alternating current (AC) in electrocoagulation processes. The main objective of this study is to investigate the effect of AC on the removal efficiency of iron using zinc as anode and cathode. The effect of the initial concentration of iron, pH, temperature, current density and coexisting ions were investigated. The adsorption kinetics of iron on zinc hydroxide is also studied. For this, equilibrium adsorption behaviour is analysed by fitting the Langmuir and Freundlich isotherm models. The adsorption kinetics of electrocoagulation was analysed using first, second order kinetic models. Finally, the effects of temperature were studied to determine the nature of adsorption.

EXPERIMENTAL SECTION

Cell Construction and Electrolysis

The electrolytic cell (Figure 1) consisted of a 1.0 – L Plexiglas vessel that was fitted with a polyvinylchloride (PVC) cell cover with slots to introduce the electrodes, pH sensor, a thermometer and the electrolytes. Zinc (commercial grade, India), with a surface area of 0.2 dm^2 acted as the anode and cathode, respectively, and placed at an interelectrode distance of 0.005 m. The temperature of the electrolyte was controlled to the desired value with a variation of ±2 K by adjusting the rate of flow of thermostatically controlled water through an external glass-cooling spiral. A regulated direct current (DC) was supplied from a rectifier

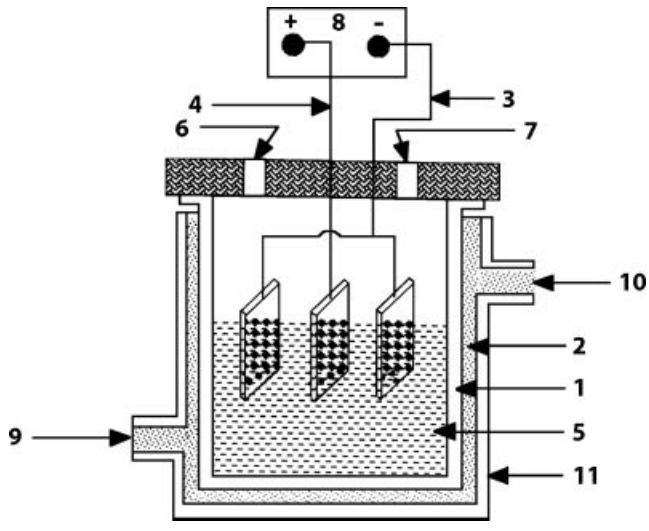

Figure 1. Laboratory scale Cell Assembly: (1) Cell, (2) thermostatic water, (3) cathode, (4) anode, (5) electrolyte, (6,7) holes to introduce pH sensor and thermometer, (8) DC source, (9) inlet of thermostatic water, (10) outlet of thermostatic water and (11) thermostat.

(10 A, 0–25 V; Aplab Model, Chennai, India) and regulated alternating current (AC) was supplied from a source (0–5 A, 0–270 V, 50 Hz; AMETEK – Model: EC1000 S, Berwyn).

The iron ($Fe(SO_4)$, Analar Reagent, Merck, Germany) was dissolved in water for the required concentration. A 0.90 L portion of solution was used for each experiment, which was used as the electrolyte. The pH of the electrolyte was adjusted, if required, with HCl and NaOH (Analar Reagent) solutions before adsorption experiments. To examine the effect of co-existing ions, for the removal of iron, sodium salts (Analar Reagent) of arsenate, phosphate, boron and fluoride were added to the electrolyte for required concentrations. All the experiments were repeated three times for reproducibility and the accuracy of the results are ±1%.

Analytical Procedure

The concentration of iron, arsenate, phosphate, boron and fluoride was analysed using UV–Visible Spectrophotometer (MERCK, Spectroquant Pharo 300, Darmstadt, Germany) using standard MERCK analysis KIT. The SEM and EDAX of iron adsorbed zinc hydroxide coagulant were analysed with a Scanning Electron Microscope (Hitachi, Japan – Model s-3000 h).

RESULTS AND DISCUSSION

Effect of Current Density

It is well known that the current density is the very important factor for electrocoagulation process. The amount of iron removal and removal rate has increased by increasing current density. Further, the amount of iron removal depends upon the quantity of adsorbent (zinc hydroxide) generated, which is related to the time and current density. The amount of adsorbent ($Zn(OH)_2$) was determined from the Faraday law:

$$E_c = ItM/ZF \tag{7}$$

where I is the current (A), t is the time (s), M is the molecular weight, Z is the electron involved, and F is the Faraday constant (96 485.3 coulomb/mol). To investigate the effect of current density on the iron removal, a series of experiments were carried out by solutions containing constant iron loading of 10 mg L^{-1}, at a pH 7.0, with current density being varied from 0.02 to 0.08 A dm^{-2} using both AC and DC current source. The results showed that the optimum removal efficiency of 99.6% and 99.1% with the energy consumption of 0.625 and 0.991 kWh kL^{-1} was achieved at a current density of 0.06 A dm^{-2}, at pH of 7.0 using AC and DC, respectively. The results are presented in Table 1. The results show that the removal efficiency of iron was higher and energy consumption was lower in the case of AC than DC. This may be due to the uniform dissolution of anode and cathode during electrocoagulation in the case of AC. The removal efficiency was found showing the amount of iron adsorption increases with the increase in adsorbent concentration, which indicates that the adsorption depends up on the availability of binding sites for iron.

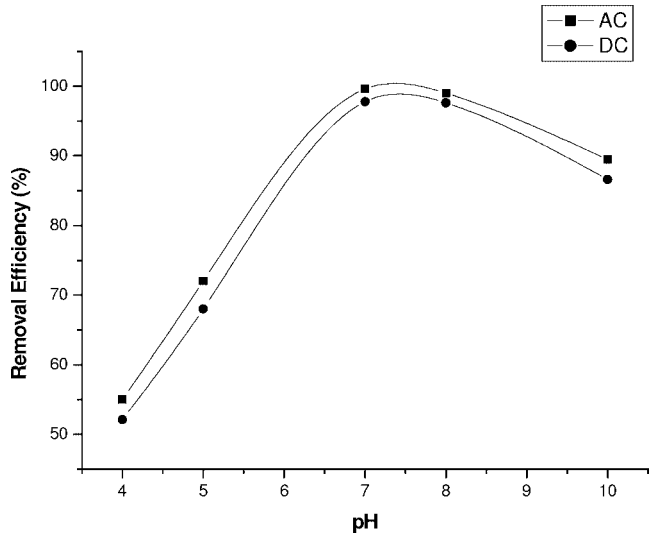

Figure 2. Effect of pH on the removal of iron.

Effect of pH

It has been established that the influent pH is an important operating factor influencing the performance of electrochemical processes. In order to examine the effect of the initial pH for AC and DC source, experiments were carried out in acidic (pH 4.0), slightly acidic (pH 5), neutral (pH 7.0), slightly neutral (pH 8), and alkaline (pH 10.0) media having 10 mg $L^{-1}$of iron containing solutions. The % of iron adsorption was maximum at pH 7, a decreasing trend in adsorption was observed when below and above pH 7 for both AC and DC source. At an initial concentration of 10 mg L^{-1}, maximum adsorption of 99.6% and 99.1% at pH 7 for AC and DC source, respectively, was observed (Figure 2). According to Zn-H_2O Pourbaix diagram (Pourbaix et al., 1966) and in thermodynamic point of view, that the precipitation of $Zn(OH)_2$ would only be significant at pH ≥ 8.6, however, the interfacial pH-increase during the electrocoagulation process favoured the zinc hydroxide formation and resulting higher removal efficiency at pH 7.0.

Effect of Initial Iron Concentration

To study the effect of initial concentration, experiments were conducted at varying initial concentrations from 5 to 25 mg L^{-1} using AC and DC. As seen from Figure 3 the adsorption of iron is

Table 1. Effect of current density on the removal efficiency of iron using AC and DC with initial iron concentration 10 mg L^{-1}

	AC		DC	
Current density (A dm^{-2})	Removal efficiency (%)	Energy consumption (kWh kL^{-1})	Removal efficiency (%)	Energy consumption (kWh kL^{-1})
0.02	93.1	0.132	92.9	0.654
0.04	96.9	0.399	96.3	0.789
0.06	99.6	0.625	99.1	0.991
0.08	99.6	0.684	99.4	1.195
0.1	99.7	0.701	99.5	1.301

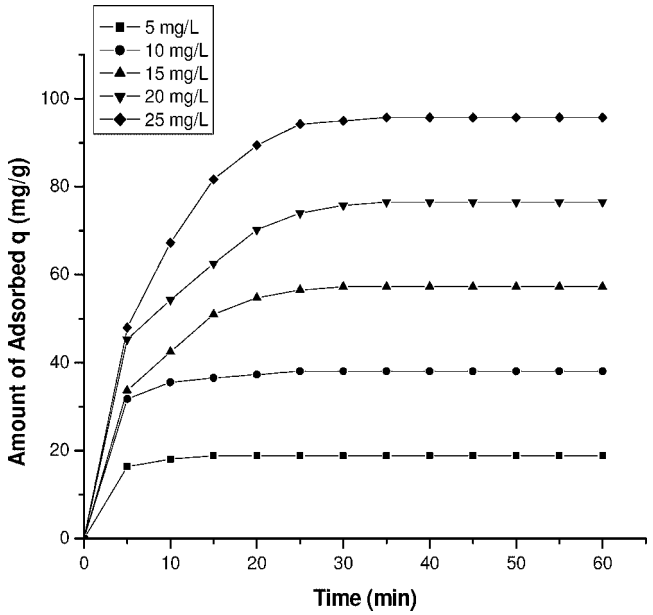

Figure 3. Effect of electrolysis time and amount of iron adsorbed.

increased with increase in iron concentration and remains constant after the equilibrium time. The equilibrium time was 30 min for all concentration studied (5–25 mg L^{-1}). The amount of iron adsorbed (q) increased from 18.66 to 93.99 mg g^{-1} as the concentration was increased from 5 to 25 mg L^{-1} for the AC source. The figure also shows that the adsorption is the rapid in the initial stages and gradually decreases with progress of adsorption. The plots are single, smooth and continuous curves leading to saturation, suggesting the possible monolayer coverage to iron on the surface of the adsorbent (Namasivayam and Prathap, 2005). In the case of DC the equilibrium time was found to be 45 min for all concentration studied (Figure not shown).

Effect of Coexisting Ions

To study the effect of co-existing ions, in the removal of iron, sodium salts of carbonate (0–250 mg L^{-1}), phosphate (0–50 mg L^{-1}), boron (0–25 mg L^{-1}), and fluoride (0–5 mg L^{-1}) was added to the electrolyte and electrolysis was carried out using AC with an initial pH of 7.

Carbonate

Effect of carbonate on iron removal was evaluated by increasing the carbonate concentration from 0 to 250 mg L^{-1} in the electrolyte. The removal efficiencies are 99.6%, 99.6%, 99.4%, 61.6%, 40.1% and 26% for the carbonate ion concentration of 0, 2, 5, 65, 150 and 250 mg L^{-1}, respectively. From the results it is found that the removal efficiency of the iron is not affected by the presence of carbonate below 5 mg L^{-1}. Significant reduction in removal efficiency was observed above 5 mg L^{-1} of carbonate concentration is due to the passivation of anode resulting, the hindering of the dissolution process of anode.

Phosphate

The concentration of phosphate ion was increased from 0 to 50 mg L^{-1}, the contaminant range of phosphate in the ground water. The removal efficiency for iron was 99.6%, 99.6%, 99.5%, 50.6% and 45.9% for 0, 2, 5, 25 and 50 mg $L^{-1}$of phosphate ion, respectively. There is no change in removal efficiency of iron below 5 mg L^{-1} of phosphate in the water. At higher concentrations (at and above 5 mg L^{-1}) of phosphate, the removal efficiency decreases to 45.9%. This is due to the preferential adsorption of phosphate over iron as the concentration of phosphate increase.

Boron

The concentration of boron ion was increased from 0 to 25 mg L^{-1}. The removal efficiency of iron was 99.6%, 99.6%, 55.4%, 50.2% and 36.3% for 0, 2, 5, 15 and 25 mg L^{-1} of boron ion, respectively. There is not much variation was observed in removal efficiency of iron up to 2 mg L^{-1} of boron in water. At higher concentrations (at and above 2 mg L^{-1}) of boron, the removal efficiency decreases to 36.3%. This is due to the preferential adsorption of boron over iron as the concentration of boron increase.

Fluoride

From the results it is found that the efficiency decreased from 99.6%, 81.6%, 64.3%, 51.6% and 18.4% by increasing the concentration of fluoride from 0, 0.2, 0.5, 2.0 and 5.0 mg L^{-1}. This is due to the preferential adsorption of fluoride over iron as the concentration of fluoride increases. So, when fluoride ions are present in the water to be treated fluoride ions compete greatly with iron for the binding sites.

Adsorption Kinetics

The adsorption kinetic data of iron are analysed using Lagergran rate equation. The first order Lagergran model is (Bina et al., 2007):

$$dq/dt = k_1(q_e - q_t) \tag{8}$$

where q_t is the amount of iron adsorbed on the adsorbent at time t (min) and k_1 (min^{-1}) is the rate constant of first order adsorption. The integrated form of the above equation is:

$$\log(q_e - q_t) = \log(q_e) - k_1 t/2.303 \tag{9}$$

where q_e is the amount of iron adsorbed at equilibrium. The q_e and rate constant (k_1) were calculated from the slope of the plots of log $(q_e - q_t)$ versus time (t). A straight line obtained from the plots suggests the applicability of this kinetic model. It was found that the calculated q_e values are not agreed with the experimental q_e values (Figure not shown). So the adsorption does not obey the first order kinetics adsorption.

The second order kinetic model is expressed as (Mckay and Ho, 1999):

$$dq/dt = k_2(q_e - q_t)^2 \tag{10}$$

where k_2 is the rate constant of second order adsorption. The integrated form of Equation (10) with the boundary condition $t = 0$ to $t > 0$ ($q = 0$ to $q > 0$) is:

$$1/(q_e - q_t) = 1/q_e + k_2 t \tag{11}$$

Equation (11) can be rearranged and linearised as:

$$t/q_t = 1/k_2 q_e^2 + t/q_e \tag{12}$$

The second order kinetic values of q_e and k_2 were calculated from the slope and intercept of the plots t/q versus t (Figure 4). Table 2 depicts the computed results obtained from first and second order kinetic model for AC and DC source. The calculated

Table 2. Comparison between the experimental and calculated q_e values for different initial iron concentrations in first and second order adsorption kinetics at temperature 305 K and pH 7

			First order adsorption			Second order adsorption		
Current source	Concentration (mg L^{-1})	q_e (exp)	q_e (Cal)	$K_1 \times 10^3$ (min mg^{-1})	R^2	q_e (Cal)	$K_2 \times 10^3$ (min mg^{-1})	R^2
AC	5	18.66	33.11	−0.0088	0.7866	18.22	0.0083	0.9999
	10	38.56	64.23	−0.0056	0.7121	37.96	0.0071	0.9997
	15	56.53	68.22	−0.0043	0.8122	56.31	0.0054	0.9988
	20	74.39	76.21	−0.0039	0.7598	73.81	0.0031	0.9976
	25	93.99	166.1	−0.0031	0.7982	94.26	0.0027	0.9998
DC	5	18.51	45.32	−0.0081	0.7954	18.44	0.0071	0.9965
	10	38.15	49.82	−0.0045	0.7325	38.07	0.0066	0.9992
	15	56.01	56.46	−0.0036	0.8022	55.79	0.0057	0.9991
	20	73.47	59.71	−0.0031	0.7623	72.94	0.0029	0.9999
	25	93.63	66.25	−0.0029	0.8147	93.01	0.0021	0.9998

q_e values well agree with the experimental q_e values for second order kinetics model better than the first order kinetics model for both AC and DC. These results indicate that the adsorption system belongs to the second order kinetic model. Similar phenomena have been observed in the adsorption of phosphate in Fe (III)/Cr (III) hydroxide (Namasivayam and Prathap, 2005).

Adsorption Isotherm

The adsorption capacity of the adsorbent has been tested using Freundlich and Langmuir isotherms. To determine the isotherms, the initial pH was kept at 7 (at 0.06 A dm^{-2}) and the concentration of iron used was in the range of 5–25 mg L^{-1} for AC and DC source.

Freundlich Isotherm

The Freundlich adsorption isotherm is represented by Namasivayam and Senthil Kumar (1998):

$$q_e = KC^n \tag{13}$$

Equation (13) can be linearised in logarithmic form and the Freundlich constants can be determined as follows (Freundlich and Uber, 1985):

$$\log q_e = \log k_f + n \log C_e \tag{14}$$

where k_f is the Freundlich constant related to adsorption capacity, n is the energy or intensity of adsorption, C_e is the equilibrium concentration of iron (mg L^{-1}). To determine the isotherms, the iron concentration used was 5–25 mg L^{-1} and at an initial pH 7. From the analysis of the results it is found that the Freundlich plots do not fit satisfactorily with the experimental data obtained in the present study (Figure not shown). This is well agreed with the results presented in the literature (Namasivayam and Prathap, 2005).

Langmuir Isotherm

Langmuir isotherm is commonly expressed as (Langmuir, 1918):

$$C_e/q_e = 1/q_0 b + C_e/q_0 \tag{15}$$

where C_e is the concentration of the iron solution (mg L^{-1}) at equilibrium, q_e is the maximum capacity to form a complete monolayer on the surface, q_0 and b is the Langmuir constant related to adsorption capacity and free energy of adsorption. When $1/q_e$ is plotted against $1/C_e$ a straight line with slope $1/q_0 b$ is obtained which shows the adsorption follow the Langmuir isotherm suggesting that the adsorption is apparently with monolayer coverage of adsorbed molecule as in Figure 5. The Langmuir plot is a better fit with the experimental data compare to Freundlich plots. The value of the adsorption capacity q_m as found to be 1456.33 and 1301.22 mg/g for AC and DC source.

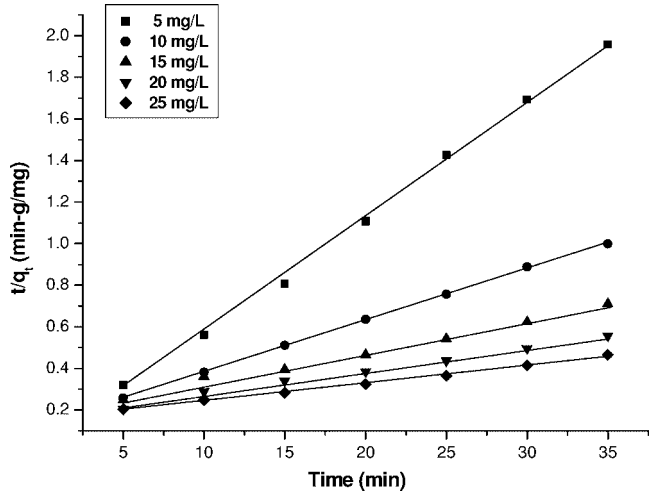

Figure 4. Second order kinetic model plot of different concentrations of iron.

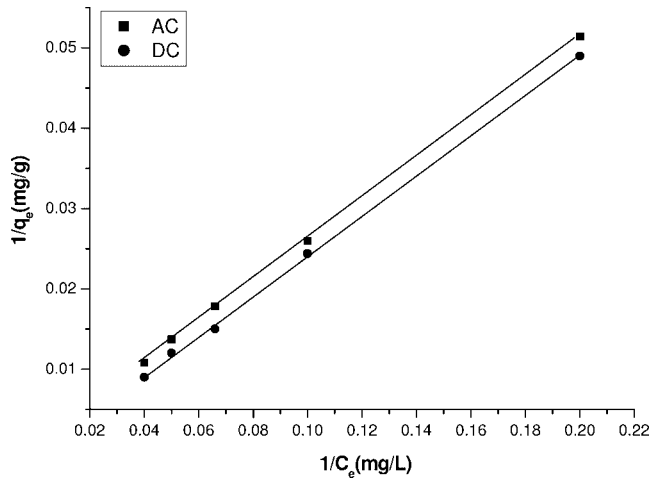

Figure 5. Plot of iron adsorbed (q_e) and concentration (C_e).

Table 3. Constant parameters and correlation co-efficient calculated for different adsorption isotherm models at room temperature for iron adsorption at 10 (mg L^{-1}) at room temperature

	Constants			
Isotherm	q_m (mg g^{-1})	b (L mg^{-1})	R_L	$R2$
Langmuir				
AC	1456.33	0.0065	0.8799	0.9999
DC	1301.22	0.0051	0.8547	0.9998
	K_f (mg g^{-1})	n (L mg^{-1})		R^2
Freundlich				
AC	1.226	1.0092		0.9864
DC	1.361	0.9923		0.9821

The essential characteristics of the Langmuir isotherm can be expressed as the dimensionless constant R_L (Michelson et al., 1975):

$$R_L = 1/(1 + bC_0) \tag{16}$$

where R_L is the equilibrium constant it indicates the type of adsorption, b, C_0 is the Langmuir constant. The R_L values between 0 and 1 indicate the favourable adsorption. The R_L values were found to be between 0 and 1 for all the concentration of iron studied. The results are presented in Table 3.

The correlation co-efficient values of different isotherm models are listed in Table 3. The Langmuir isotherm model has higher regression co-efficient ($R^2 = 0.999$) when compared to the other models. The adsorption data show good fit to the Langmuir then Freundlich as depicted by the regression coefficient for these systems for both AC and DC. R_L values between 0 and 1.0 further indicate a favourable adsorption of iron.

Effect of Temperature

The amount of iron adsorbed on the adsorbent increases by increasing the temperature indicating the process to be endothermic (Nayak Preeti et al., 2007). The diffusion co-efficient (D) for intraparticle transport of iron species in to the adsorbent particles has been calculated at different temperature by:

$$t_{1/2} = 0.03 \times {r_o}^2/D \tag{17}$$

where $t_{1/2}$ is the time of half adsorption (s), r_o is the radius of the adsorbent particle (cm), D is the diffusion co-efficient in $cm^2\ s^{-1}$. For all chemisorption system the diffusivity co-efficient should be 10^{-5} to $10^{-13}\ cm^2\ s^{-1}$ (Yang and Bushra, 2001). In the present work, D is found to be in the range of $10^{-7}\ cm^2\ s^{-1}$. The pore diffusion coefficient (D) values for different initial concentrations of iron and temperature are presented in Table 4.

Table 4. Pore diffusion coefficients for the adsorption of iron at various concentration and temperature

Concentration (mg L^{-1})	Pore diffusion constant $D \times 10^{-9}$ ($cm^2\ s^{-1}$)
5	1.6451
10	1.0012
15	0.9624
20	0.9465
25	0.8312
Temperature (K)	**Pore diffusion constant $D \times 10^{-9}$ ($cm^2\ s^{-1}$)**
313	1.0012
323	1.0193
333	1.9946
343	2.1351

To find out the energy of activation for adsorption of iron, the second order rate constant is expressed in Arrhenius form (Golder et al., 2006):

$$\ln k_2 = \ln k_o - E/RT \tag{18}$$

where k_o is the constant of the equation (g/mg/min), E is the energy of activation (J mol^{-1}), R is the gas constant (8.314 J $mol^{-1}\ K^{-1}$) and T is the temperature (K). Table 5 shows that the rate constants vary with temperature according to Equation (18). The activation energy is 11.03 and 9.96 kJ mol^{-1} for AC and DC, respectively, is calculated from slope of $\log k_2$ versus $1/T$ (Figure not shown). The free energy change is obtained using the following relationship:

$$\Delta G^o = -RT \ln K_c \tag{19}$$

where $\triangle G^\circ$ is the free energy (kJ mol^{-1}), K_c is the equilibrium constant, R is the gas constant and T is the temperature (K). The K_c and $\triangle G^\circ$ values are presented in Table 5. From the table it is found that the negative value of $\triangle G^\circ$ indicates the spontaneous nature of adsorption.

Other thermodynamic parameters such as entropy change ($\triangle S^\circ$) and enthalpy change ($\triangle H^\circ$) were determined using van't Hoff equation:

$$\ln K_c = \frac{\Delta S}{R} - \frac{\Delta H}{RT} \tag{20}$$

The enthalpy change ($\triangle H^\circ$) and entropy change ($\triangle S^\circ$) were obtained from the slope and intercept of the van't Hoff linear plots of $\ln K_c$ versus $1/T$ (Figure 6). A positive value of enthalpy change ($\triangle H^\circ$) indicates that the adsorption process is endothermic in

Table 5. Thermodynamic parameters for the adsorption of iron

	AC				DC			
Temperature (K)	K_c	$\triangle G^\circ$ (J mol^{-1})	$\triangle H^\circ$ (kJ mol^{-1})	$\triangle S^\circ$ (J $mol^{-1}\ K^{-1}$)	K_c	$\triangle G^\circ$ (J mol^{-1})	$\triangle H^\circ$ (kJ mol^{-1})	$\triangle S^\circ$ (J $mol^{-1}\ K^{-1}$)
313	1.2251	−0.1921	5.993	10.623	1.2531	−0.0661	6.003	10.112
323	1.2463	−0.2011			1.2698	−0.0997		
333	1.2677	−0.3651			1.2964	−0.1864		
343	1.3321	−0.3754			1.3021	−0.2654		

Table 6. Comparison between the experimental and calculated q_e values for different initial iron concentrations of 10 (mg L^{-1}) in first and second order adsorption isotherm at various temperatures and pH 7

		First order adsorption			Second order adsorption		
Temperature (K)	q_e (exp)	q_e (Cal)	K_1 (min mg^{-1})	R^2	q_e (Cal)	K_2 (min mg^{-1})	R^2
313	38.66	38.64	−0.0033	0.7886	38.59	0.1556	0.9996
323	38.72	38.69	−0.0029	0.7987	38.62	0.1664	0.9965
333	38.85	38.77	−0.0027	0.7614	38.77	0.2055	0.9978
343	38.91	38.84	−0.0026	0.7754	38.85	0.3641	0.9935

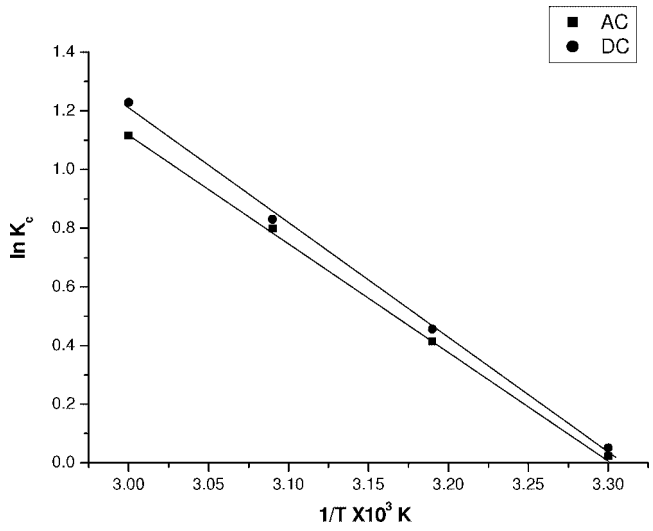

Figure 6. Plot of ln K_c and $1/T$.

nature (Namasivayam and Prathap, 2005), and the negative value of change in internal energy ($\triangle S^\circ$) show the spontaneous adsorption of iron on the adsorbent. Positive values of entropy change show the increased randomness of the solution interface during the adsorption of iron on the adsorbent (Table 6). Enhancement of adsorption capacity of electrocoagulant (Zinc hydroxide) at higher temperatures may be attributed to the enlargement of pore size and or activation of the adsorbent surface. Using Lagergran rate equation, first-order rate constants and correlation co-efficient were calculated for different temperatures (305–343 K). The calculated 'q_e' values obtained from the first order kinetics do not agree with the experimental 'q_e' values. Second-order kinetics model shows that the calculated 'q_e' values agree with the experimental values (Table 6). This indicates that the adsorption follows second order kinetic model at different temperatures used in this study. From the table, it is found that the rate constant 'k_2' increased with increasing the temperature from 305 to 343 K. The increase in adsorption may be due to change in pore size on increase in kinetic energy of the iron species and the enhanced rate of intraparticle diffusion of adsorbate.

A Pilot Plant Study

A pilot plant capacity cell (Figure 7) was designed, fabricated and operated for the removal of iron from water. The system consists of a AC/DC power supply, an electrochemical reactor, a water tank, a feed pump, a flow control valve, a flow measuring unit, a circulation pump, settling tank, sludge collection tank, filtration unit provisions for gas outlet and treated water outlet. The reactor is made of PVC with an active volume of 1000 L. The zinc electrodes (anode and cathode) each consist of five pieces situated approximately 5 mm apart from each other and submerged in the solution. The total electrode surface area is 1500 cm^2 for both cathodes and anodes. The cell was operated at a current

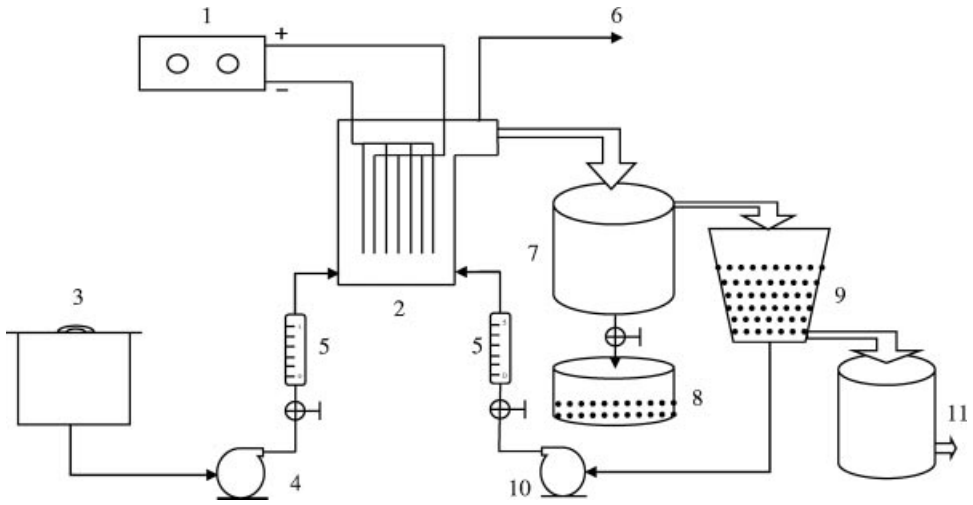

Figure 7. Flow diagram of the pilot plant electrocoagulation system. (1) DC power supply, (2) electrocoagulation cell, (3) water tank, (4) inlet pump, (5) flow meter, (6) gas outlet, (7) setting tank, (8) sludge collection tank, (9) filtration unit, (10) recirculation pump and (11) treated water.

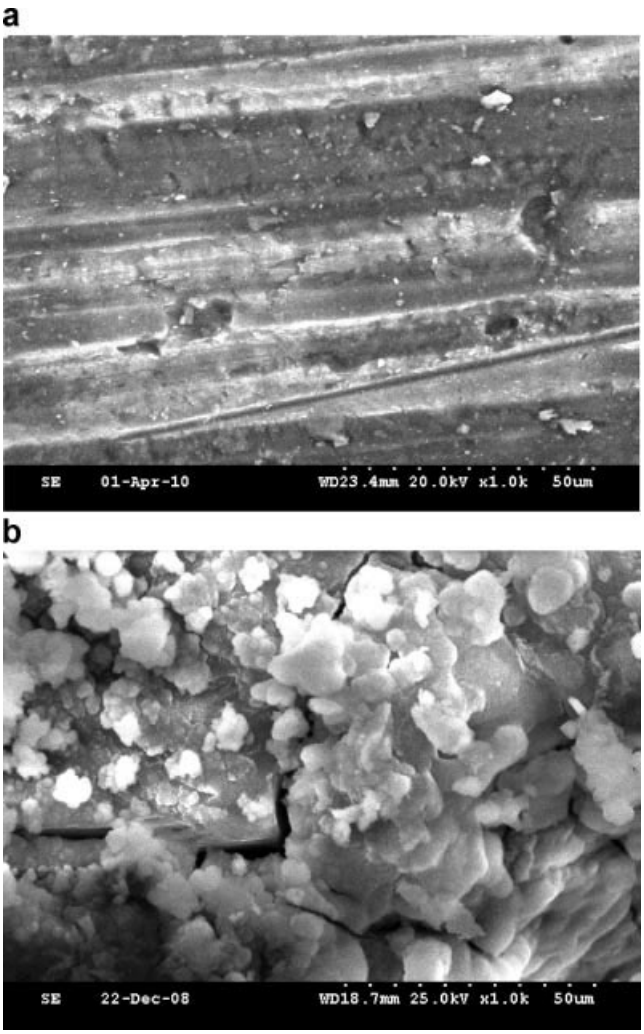

Figure 8. SEM image of the anode (a) before and (b) after treatment.

density of 0.06 A dm^{-2} and the electrolyte pH of 7.0. The results showed that the optimum removal efficiency of 99.6% and 99.1% with the energy consumption of 0.625 and 0.991 kWh kL^{-1} was achieved at a current density of 0.06 A dm^{-2}, at pH of 7.0 using AC and DC, respectively. The results were consistent with the results obtained from the laboratory scale, showing that the process was technologically feasible.

SEM and EDAX Studies

In order to gain more insight into the effect of alternating current, the morphology of the electrode surface after two kinds of electrolysis (AC and DC) was characterised by SEM as shown in Figure 8(a) and (b). It can be observed that when the AC was fed, less disordered pores formed and a smooth microstructure of zinc suggesting the zinc electrodes were dissolved uniformly during the electrolysis. While for the electrodes fed with DC, the electrode surface is found to be rough, with a number of dents. These dents are formed around the nucleus of the active sites where the electrode dissolution results in the production of zinc hydroxides. The formation of a large number of dents may be attributed to the anode material consumption at active sites due to the generation of oxygen at its surface.

Energy-dispersive analysis of X-rays was used to analyse the elemental constituents of iron-adsorbed zinc hydroxide shown in Figure 9. It shows that the presence of Fe, Zn and O appears in the spectrum. EDAX analysis provides direct evidence that iron is adsorbed on zinc hydroxide. Other elements detected in the adsorbed zinc hydroxide come from adsorption of the conducting electrolyte, chemicals used in the experiments, alloying and the scrap impurities of the anode and cathode.

CONCLUSIONS

The results showed that the optimised removal efficiency of 99.6% and 99.1% was achieved for AC and DC source at a current density of 0.006 A dm^{-2} and pH of 7.0 using zinc as anode and cathode. The zinc hydroxide generated in the cell remove the iron present in the water and to reduce the iron concentration to less than 0.3 mg L^{-1}, and made it for drinking. The pilot scale results showing that the process was technologically feasible. For

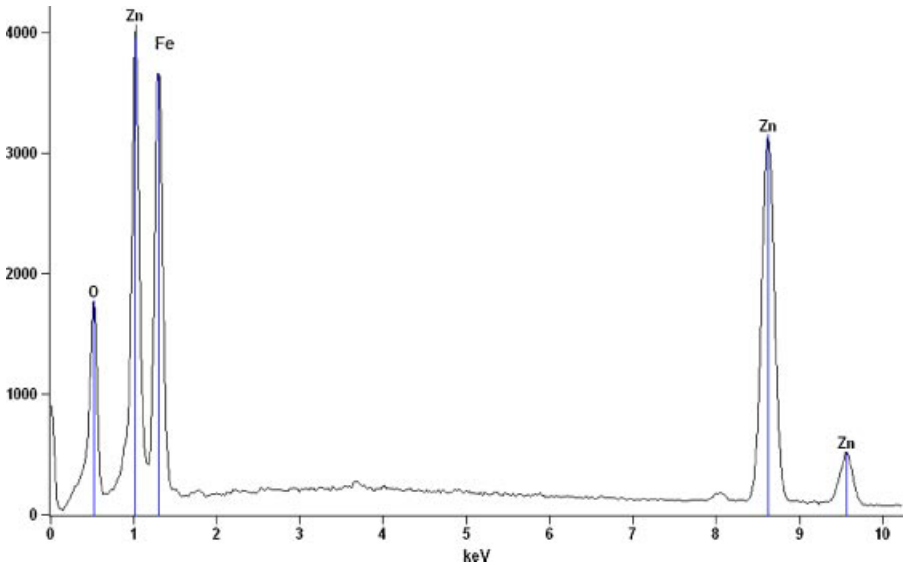

Figure 9. EDAX for iron adsorbed electrocoagulant.

both AC and DC electrolysis the adsorption of iron preferably fitting the Langmuir adsorption isotherm. The adsorption process follows second order kinetics. Temperature studies showed that adsorption was endothermic and spontaneous in nature. From the surface characterisation studies, it is confirmed that the zinc hydroxide generated in the cell adsorbed iron present in the water.

ACKNOWLEDGEMENTS

The author wish to express their gratitude to the Director, Central Electrochemical Research Institute, Karaikudi, for publishing this article.

REFERENCES

Adhoum, N. and L. Monser, "Decolourisation and Removal of Phenolic Compounds From Olive Mill Wastewater by Electrocoagulation," Chem. Eng. Process. **43**, 1281–1287 (2004).

Ali, I. and K. K. Gupta, "Removal of Endosulfan and Methoxychlor from Water on Carbon Slurry," Environ. Sci. Technol. **42**, 766–770 (2008).

Ali, I. and V. K. Gupta, "Advances in Water Treatment by Adsorption Technology," Nature Protocols **1**, 2661–2667 (2009).

Andersen, W. C. and T. J. Bruno, "Application of Gas–Liquid Entraining Rotor to Supercritical Fluid Extraction: Removal of Iron (III) From Water," Anal. Chim. Acta **485**, 1–8 (2003).

Aziz, H. A., M. S. Yusoff, M. N. Adlan, N. H. Adnan and S. Alias, "Physicochemical Removal of Iron From Semiaerobic Landfill Leachate by Limestone Filter," Water Manage. **24**, 353–358 (2004).

Berbenni, P., A. Pollice, R. Canziani, L. Stabile and F. Nobili, "Removal of Iron and Manganese From Hydrocarbon-Contaminated Groundwaters," Bioresour. Technol. **74**, 109–114 (2002).

Bina, G., I. Begum Zareena and R. Garima, "Equilibrium and Kinetic Studies for the Adsorption of Mn(II) and Co (II) From Aqueous Media using Agar-Agar as Sorbent," Res. J. Chem. Environ. **11**, 16–21 (2007).

Carlesi Jara, C., D. Fino, V. Specchia, G. Saracco and P. Spinelli, "Electrochemical Removal of Antibiotics From Wastewaters," Appl. Catal. B **70**, 479–487 (2007).

Carlos, A., M. Huitle and S. Ferro, "Electrochemical Oxidation of Organic Pollutants for the Wastewater Treatment: Direct and Indirect Processes," Chem. Soc. Rev. **35**, 1324–1340 (2006).

Central Pollution Control Board, Ministry of Environment and Forests, www.cpcb.nic.in. Government of India, Delhi (2010).

Cho, B. Y., "Iron Removal Using Aerated Granular Filter," Process Biochem. **40**, 3314–3320 (2005).

Chen, G., "Electrochemical Technologies in Wastewater Treatment," Sep. Purif. Technol. **38**, 11–41 (2004).

Chen, X., G. Chen and P. L. Yue, "Investigation on the Electrolysis Voltage of Electrocoagulation," Chem. Eng. Sci. **57**, 2449–2455 (2002).

Christensen, P. A., T. A. Egerton, W. F. Lin, P. Meynet, Z. G. Shaoa and N. G. Wright, "A Novel Electrochemical Device for the Disinfection of Fluids by OH Radicals," Chem. Commun. **38**, 4022–4023 (2006).

Das, B., J. Talukdar, S. Sarma, B. Gohain, R. K. Dutta and A. C. Das, "Fluoride and Other Inorganic Constituents in Groundwater of Guwahati, Assam, India," Curr. Sci. **85**, 657–661 (2003).

Das, B., P. Hazarika, G. Saikia, H. Kalita, D. C. Goswami, H. B. Das, S. N. Dube and R. K. Dutta, "Removal of Iron by Groundwater by Ash: A Systematic Study of a Traditional Method," J. Hazard. Mater. **141**, 834–841 (2007).

Ellis, D., C. Bouchard and G. Lantagne, "Removal of Iron and Manganese From Groundwater by Oxidation and Microfiltration," Desalination **130**, 255–264 (2000).

Freundlich, H. and M. Uber, "Die adsorption in Losungen," Z. Phys. Chem. **57**, 387–389 (1985).

Gabrielli, C., G. G. Maurin, H. Francy-Chausson, P. Thery, T. T. M. Tran and M. Tlili, "Electrochemical Water Softening: Principle and Application," Desalination **201**, 150–163 (2006).

Golder, A. K., A. N. Samantha and S. Ray, "Removal of Phosphate From Aqueous Solution Using Calcined Metal Hydroxides Sludge Waste Generated From Electrocoagulation," Sep. Purif. Technol. **52**, 102–109 (2006).

Gupta, V. K. and A. Rastogi, "Biosorption of Lead From Aqueous Solutions by Non-Living Algal Biomass Oedogonium sp. and Nostoc sp. – A Comparative Study," Coll. Surfaces B **64**, 170–178 (2008).

Gupta, V. K. and A. Suhas, "Application of Low Cost Adsorbents for Dye Removal – A Review," J. Environ. Manage. **90**, 2313–2342 (2009).

Gupta, V. K., P. J. M. Carrott, M. M. L. Ribeiro Carrott and A. Suhas, "Low Cost Adsorbents: Growing Approach to Wastewater Treatment – A Review," Crit. Rev. Environ. Sci. Technol. **39**, 783–842 (2009).

Gupta, V. K., A. Mittal, L. Kurup and J. Mittal, "Adsorption of Basic Fuchsin Using Waste Materials – Bottom Ash and De-oiled Soya as Adsorbents," J. Colloid Interface Sci. **319**(1), 30–39 (2008).

Gupta, V. K., A. Mittal, R. Jain, M. Mathur and S. Sikarwar, "Adsorption of Safranin-T from Wastewater Using Waste Materials – Activated Carbon and Activated Rice Husk," J. Colloid Interface Sci. **303**(1), 80–86 (2006).

Ikematsu, M., K. Kaneda, M. Iseki and M. Yasuda, "Electrochemical Treatment of Human Urine for Its Storage and Reuse as Flush Water," Sci. Total Environ. **382**, 159–164 (2007).

Langmuir, I., "The Adsorption of Gases on Plane Surface of Gases on Plane Surface of Glass, Mica and Platinum," J. Am. Chem. Soc. **40**, 1361–1365 (1918).

Mahanta, D. B., N. N. Das and R. K. Dutta, "A Chemical and Bacteriological Study of Drinking Water in Tea Gardens of Central Assam," Indian J. Environ. Prot. **24**, 654–660 (2004).

Mckay, G. and Y. S. Ho, "The Sorption of Lead (II) on Peat," Water Res. **33**, 578–584 (1999).

Michelson, L. D., P. G. Gideon, E. G. Pace and L. H. Kutal, "Removal of Solute Mercury From Waste Water by Complexing Technique," US Dept. Ind. Office Water Res. Technol. Bull. **67**, 265 (1975).

Miwa, D. W., G. R. P. Malpass, S. A. S. Machado and A. J. Motheo, "Electrochemical Degradation of Carbaryl on Oxide Electrodes," Water Res. **40**, 3281–3289 (2006).

Munter, R., H. Ojaste and J. Sutt, "Complexed Iron Removal From Ground Water," J. Environ. Eng. **131**, 1014–1020 (2005).

Namasivayam, C. and K. Prathap, "Recycling Fe (III)/Cr (III) Hydroxide, an Industrial Solid Waste for the Removal of Phosphate From Water," J. Hazard. Mater. **123B**, 127–134 (2005).

Namasivayam, C. and S. Senthil Kumar, "Removal of Arsenic (V) From Aqueous Solutions Using Industrial Solid Waste: Adsorption Rates and Equilibrium Studies," Ind. Eng. Chem. Res. **37**, 4816–4822 (1998).
Nayak Preeti, S. and B. K. Singh, "Sorption Dynamics of Phenol on Naturally Occurring Low Cost Clay," Res. J. Chem. Environ. **11**, 23–28 (2007).
Official Journal of the European Communities, Council Directive 98/83/EC on the Quality of Water Intended for Human Consumption. L330/32–L330/50 (1998).
Onder, E., A. S. Koparal and U. B. Ogutveren, "An Alternative Method for the Removal of Surfactants From Water: Electrochemical Coagulation," Sep. Purif. Technol. **52**, 527–532 (2007).
Pourbaix, M. and J. Vanmuylder, in "Atlas of Electrochemical Equilibria in Aquous Solutions: Zinc" J. Vanmuylder, M. Pourbaix, Eds., Pergamon, New York (1966) 409.
Sharma, R., S. Shah and C. Mahanta, "Hydrogeochemical Study of Groundwater Fluoride Contamination: A Case Study From Guwahati City," India Asian J. Water Environ. Pollut. **2**, 47–54 (2005).
Subba Rao, N., "Iron Content in Groundwaters of Visakhapatnam Environs, Andhra Pradesh, India," Environ. Monit. Assess **136**, 437–447 (2007).
Vaaramaa, K. and H. J. Lehto, "Removal of Metals and Anions From Drinking Water by Ion Exchange," Desalination **155**, 157–170 (2003).
WHO Guidelines for Drinking Water Quality, "Health Criteria and Other Supporting Information," 2nd ed., (2), WHO, Geneva (1996).
Yang, X. Y. and A. D. Bushra, "Application of Branched Pore Diffusion Model in the Adsorption of Reactive Dyes on Activated Carbon," Chem. Eng. J. **83**, 15–23 (2001).

Manuscript received April 1, 2011; revised manuscript received May 6, 2011; accepted for publication May 25, 2011.